ELSEVIER

Chemical Engineering Journal 140 (2008) 632–637

Chemical Engineering Journal

www.elsevier.com/locate/cej

Short communication

$SrMoO_4$ powders processed in microwave-hydrothermal: Synthesis, characterization and optical properties

J.C. Sczancoski [a,*], L.S. Cavalcante [a], M.R. Joya [a], J.A. Varela [b], P.S. Pizani [a], E. Longo [b]

[a] *LIEC, Departamento de Química e Física da Universidade Federal de São Carlos, P.O. Box 676, 13565-905 São Carlos, SP, Brazil*
[b] *Departamento de Físico-Química-IQ, Universidade Estadual Paulista, P.O. Box 355, 14801-907 Araraquara, SP, Brazil*

Received 24 October 2007; received in revised form 3 January 2008; accepted 4 January 2008

Abstract

In this work, we report on the synthesis of $SrMoO_4$powders by co-precipitation method and processed in a microwave-hydrothermal at 413 K for 5 h. These powders were analyzed by X-ray diffraction (XRD), Fourier transform Raman (FT-Raman), ultraviolet–visible (UV–vis) absorption spectroscopy and photoluminescence (PL). XRD analyses revealed that the $SrMoO_4$ powders are free of secondary phases and crystallize in a tetragonal structure. FT-Raman investigations showed the presence of Raman-active vibration modes correspondent for this molybdate. UV–vis technique was employed to determine the optical band gap of this material. $SrMoO_4$ powders exhibit an intense PL emission at room temperature with maximum peak at 540 nm (green region) when excited by 488 nm wavelength of an argon ion laser.

Keywords: Co-precipitation; Microwave-hydrothermal; $SrMoO_4$; Optical band gap; Photoluminescence

1. Introduction

In recent years, tungstates and molybdates are materials that have attracted the interest of many technological fields and scientific areas owing to their wide potential to industrial application, including optic fiber, humidity sensor, catalysts, scintillation detector, solid-state lasers, photoluminescent devices, microwave applications and so on [1–10]. These materials have been prepared in both powder and film forms by means of several technologies, such as spray pyrolysis, pulsed laser deposition, RF-magnetron sputtering and sol–gel method [11–15]. However, these methods generally require expensive and sophisticated equipments, high temperatures for a long time, expensive precursors and high consumption of electric energy [16]. A possible alternative for reduction of these factors can be the use of hydrothermal processing methods. The conventional hydrothermal process (CH) is an efficient low temperature method that allows the formation of powders with high degree of crystallinity and with easy dispersion in an aqueous medium [17]. In contrast, the main drawback of this technique is the slow reaction kinetic at any given temperature [18]. The use of microwave energy in conventional hydrothermal system promoted the development of a new technique able to allow a rapid heating to the required temperature with rapid rates of crystallization [19]. In microwave-hydrothermal (MH) processing the factor "acceleration of chemical reaction" is promoted by high-frequency electromagnetic radiation (2.45 GHz) that interacts with the permanent dipole of the liquid phase, which initiates rapid heating from the resultant molecular rotation. Likewise, permanent or induced dipoles in the dispersed phase cause rapid heating of the particles. These result in a reaction temperature in excess of the surrounding liquid-localized superheating [19]. Therefore, MH process offer the following advantages over the CH, such as: (a) the kinetics of the reaction is enhanced by one to two orders of magnitude, (b) novel phases, especially layered ones can be obtained and (c) rapid heating to treatment temperature saves time and energy [20,21].

Recently, Thongtem et al. [22] has been reported the use of a simple and attractive method by cyclic microwave radiation. They focused on the use of microwave in solutions for fast formation of several molybdates with scheelite-type structure. The obtained results for these authors revealed different morphologies for each molybdate using the same experimental conditions. Another interesting work, Thongtem et al. [23] mentioned the preparation of $SrWO_4$ using the same experimental technique by cyclic microwave radiation. The purpose of this work was

* Corresponding author. Tel.: +55 16 3361 5215.
E-mail address: jcsfisica@gmail.com (J.C. Sczancoski).

1385-8947/$ – see front matter © 2007 Elsevier B.V. All rights reserved.
doi:10.1016/j.cej.2008.01.015

investigate the influence of pH, microwave powers and prolonged times on the structural, morphologic and optical properties of $SrWO_4$ powders.

In the present communication, we report on the preparation of $SrMoO_4$ powders by co-precipitation method and processed in a microwave-hydrothermal at 413 K for 5 h. These powders were characterized by X-ray diffraction (XRD) and Fourier transform Raman (FT-Raman). Optical properties were investigated by ultraviolet–visible (UV–vis) absorption spectroscopy and photoluminescence (PL).

2. Experimental procedure

2.1. Synthesis and microwave-hydrothermal processing of $SrMoO_4$ powders

$SrMoO_4$ powders were obtained by co-precipitation and processed in a microwave-hydrothermal with the presence of polyethylene glycol (PEG). The typical synthesis procedure is described as follows: 5×10^{-3} mol of molybdic acid (H_2MoO_4) (85% purity, Synth), 5×10^{-3} mol of strontium acetate [$(CH_3CO_2)_2Sr$] (99.5% purity, Aldrich) and 0.1 g of PEG (Mw 200) (99.9% purity, Aldrich) were dissolved in 150 mL of deionized water. Then 5 mL of ammonium hydroxide (NH_4OH) (30% in NH_3, Synth) was added in the solution until the pH value reached to 12. Afterwards, the aqueous solution was stirred for 30 min in ultrasound at room temperature. In the sequence, the mixture was transferred into a Teflon autoclave. The autoclave was then sealed and placed into a microwave-hydrothermal (2.45 GHz, maximum power of 800 W). The MH conditions were kept at 413 K for 5 h, using a heating rate fixed at 298 K/min. The pressure into the autoclave was stabilized at 294 kPa. After microwave-hydrothermal treatment, the autoclave was cooled to room temperature. The resultant solution was washed with deionized water several times to neutralize the pH of the solution (~ 7) and the white precipitates were finally collected. The obtained powders were dried in a conventional furnace at 373 K for 24 h. Four samples of $SrMoO_4$ powders were prepared using the same experimental conditions, to analyze the reproducibility of the method.

2.2. Characterizations

The obtained powders were structurally characterized by X-ray diffraction (XRD) using a Rigaku-DMax/2500PC with Cu K α radiation (λ = 1.5406 Å) in the 2θ range from 10 to 75° with 0.02°/min. Fourier transform Raman (FT-Raman) spectroscopy measurements were performed using a Bruker-RFS/100. The 1064 nm line of an Nd:YAG ion laser was used as excitation source, the power was kept at 55 mW. Ultraviolet–visible (UV–vis) spectroscopy for the spectra of optical reflectance of $SrMoO_4$ powders was taken using Cary 5G equipment. Photoluminescence (PL) measurements of the powders were taken with a U1000 Jobin-Yvon double monochromator coupled to a cooled GaAs photomultiplier and a conventional photon counting system. The 488.0 nm excitation wavelength of an argon ion laser was used with the laser's maximum output power kept at 30 mW. A cylindrical lens was used to prevent the sample from overheating. The slit width used was 100 μm. All measurements were performed at room temperature.

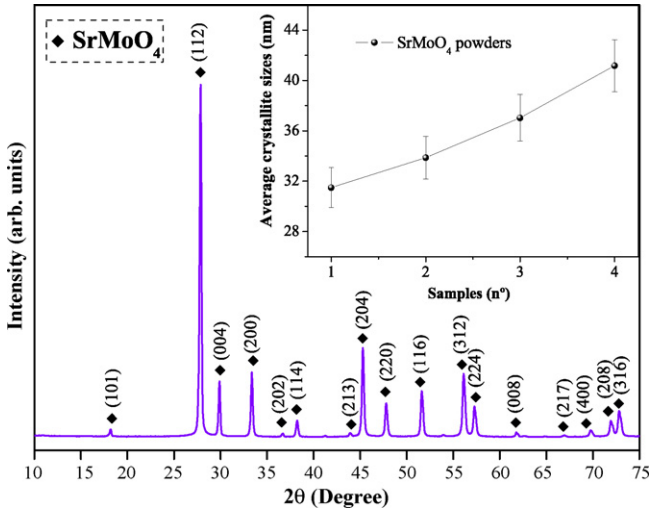

Fig. 1. XRD patterns of $SrMoO_4$ powders obtained by the microwave-hydrothermal at 413 K for 5 h. The inset shows the average crystallite size for four $SrMoO_4$ powders. The vertical bars (mean error standard).

3. Results and discussion

3.1. X-ray diffraction analysis

Fig. 1 shows a typical XRD pattern of $SrMoO_4$ powders processed in a microwave-hydrothermal at 413 K for 5 h.

All diffraction peaks can be indexed as a pure tetragonal structure with space group $I4_1/a$. The peaks indicate that the powders are well crystallized. The lattice parameters were calculated using the least square refinement from the UnitCell-97 program [24]. The obtained lattice parameters were $a = b = 5.3796$ Å and $c = 11.9897$ Å, with volume unit cell of 346.9920 Å^3. These values are in agreement with the reported data in the respective JCPDS (Joint Committee on Powder Diffraction Standards) card N^{o}08-0482 [25]. The average crystallite size was approximately estimated by the Scherrer's equation using the full width at half maximum (FWHM) of the most intense peak (1 1 2). As reported in the literature [18], the Scherrer's equation (Eq. (1)) is described as follows:

$$D = \frac{0.9\lambda}{B\cos\theta} \quad (1)$$

where λ is the wavelength of Cu-Kα (1.54059 Å), θ is the angle of Bragg diffraction and B is the FWHM. Based on this equation, the average crystallite size in the four samples of $SrMoO_4$ powders was obtained in the range from 31.49 to 41.16 nm.

3.2. Unit cell representation for $SrMoO_4$

$SrMoO_4$ crystallizes in a tetragonal structure and belong to the materials group with scheelite-type structure with space

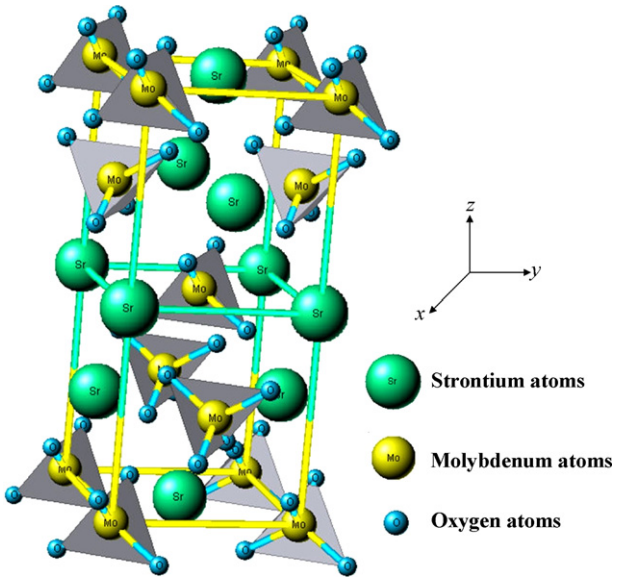

Fig. 2. 1 × 1 × 1 unit cell of $SrMoO_4$ tetragonal structure.

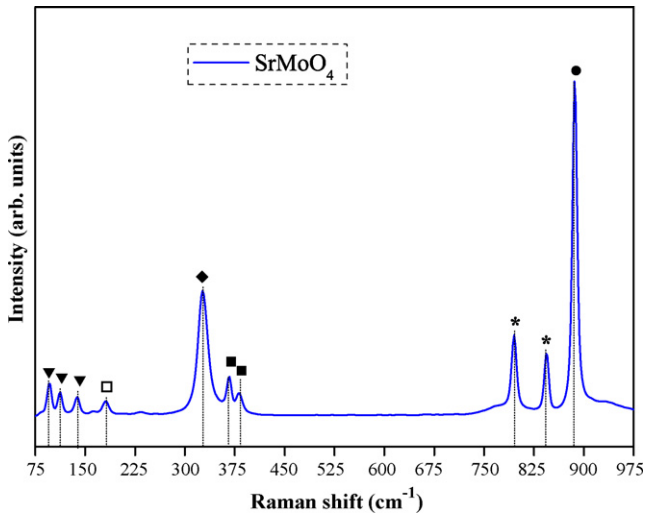

Fig. 3. Raman spectra of $SrMoO_4$ powders excited with a 1064 nm line of an Nd:YAG ion laser at room temperature. The symbols represent the assignments, Raman modes: (▼) external modes $MoO_4^{2-}$and Sr^{2+} motions, (□) fr(F_1) free rotation, (♦)$\nu_2(E)$, (■)$\nu_4(F_2)$, (∗)$\nu_3(F_2)$ and (●)$\nu_1(A_1)$.

group $I\,4_1/a$ [26,27]. Chen et al. [27] described the primitive unit cell of this structure with two $SrMoO_4$ units, each with an inversion center. The authors also mentioned that Sr and Mo sites present S_4 point symmetry. Therefore, unit cell of $SrMoO_4$ presents the molybdenum atoms surrounded by four oxygen atoms in a tetrahedral configuration and the strontium atoms surrounded by eight oxygen atoms [26,27]. Fig. 2 illustrates the representation of $SrMoO_4$ unit cell using the Java Structure Viewer Program (Version 1.08lite for Windows) [28]. The construction of this unit cell was based on the models presented by Takai et al. [29] and Grmen et al. [30] and employing the obtained lattice parameters by XRD ($a = b = 5.3796$ Å and $c = 11.9897$ Å) with the atomic coordinates listed in Table 1.

3.3. Fourier transform Raman analysis

According to Basiev et al. [31], the vibrational modes in Raman spectra of molybdates are classified into two groups, internal and external. The internal vibrations are related to the $[MO_4]^{2-}$molecular group with a stationary mass center. The external vibrations or lattice phonons are associated to the motion of the Sr^{2+}cation and the rigid molecular units. In the free space $[MO_4]^{2-}$ tetrahedrons presents T_d-symmetry. In this case, the vibrations of the $[MO_4]^{2-}$ ions are constituted by four internal modes (ν_1 (A_1), ν_2 (E), ν_3 (F_2) and ν_4 (F_2)), one free rotation mode (ν_{fr} (F_1)) and one translation mode (F_2). When the $[MO_4]^{2-}$ ions are present in a scheelite-type structure, its point symmetry reduce to S_4. Therefore, all degenerative vibrations are split due to the crystal field effect. For a tetragonal scheelite primitive cell with $K = 0$ wavevector, the results estimated by the group-theory show the presence of 26 different types of vibrations, represented by Eq. (2)[31]:

$$\Gamma = 3A_g + 5A_u + 5B_g + 3B_u + 5E_g + 5E_u \quad (2)$$

All the vibrations A_g, B_g and E_g are Raman-active where 4 A_u and 4 E_u modes are active only in infrared frequencies. The system still includes the acoustic vibrations (1A_u and 1 E_u) and the silent modes (3 B_u).

The Raman modes obtained for $SrMoO_4$ in the present work are shown in Fig. 3. As can be seen, just 10 different vibrations were detected. The internal modes $\nu_1(A_g)$, $\nu_2(E_g)$, $\nu_3(E_g)$ and $\nu_4(B_g)$ were observed at 885, 844, 795, 383, 387 and 326 cm^{-1}. The free rotation mode was detected at 180 cm^{-1} and the external modes were localized at range 96–137 cm^{-1}. These results are in agreement with that reported in the literature [22,31,32].

Table 1
Atomic coordinates used to model the tetragonal $SrMoO_4$ unit cell

Atom	Site	x	y	z
Molybdenum	4a	0	0	0
Strontium	4b	0	0	0.5
Oxygen	16f	0.233	0.140	0.820

3.4. Ultraviolet-visible absorption spectroscopy analysis

Fig. 4 shows the absorbance spectral dependence for $SrMoO_4$ powders processed in a microwave-hydrothermal at 413 K for 5 h.

The equation proposed by Wood and Tauc [33] was used to estimate the optical band gap. According to these authors, the optical band gap energy is related with absorbance and photon energy by Eq. (3):

$$h\nu\alpha \propto (h\nu - E_g^{opt})^2 \quad (3)$$

where α is the absorbance, h is the Planck constant, ν is the frequency and E_g^{opt} is the optical band gap.

Therefore, the optical band gap was determined by extrapolation of the linear portion of the curve or tail. The band gap in the materials is related with absorbance and photon energy. Therefore, the combination between absorbance and photolumi-

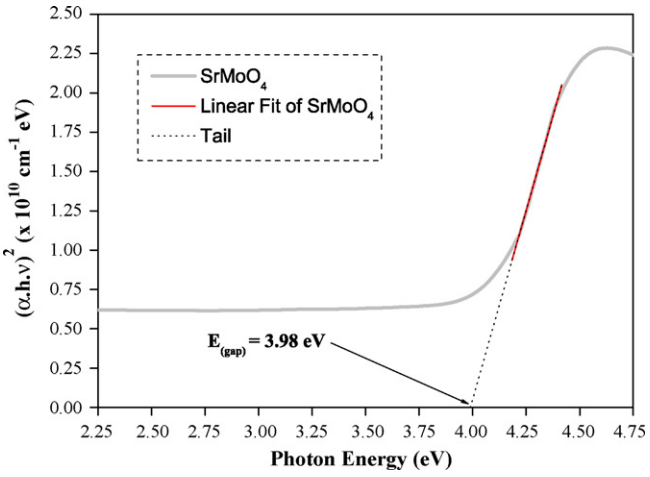

Fig. 4. UV–vis absorbance spectra at room temperature for the $SrMoO_4$ powders processed in microwave-hydrothermal at 413 K for 5 h.

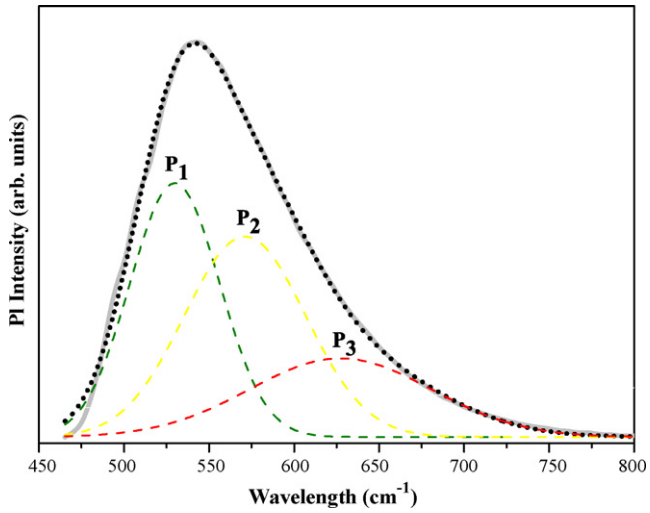

Fig. 5. Photoluminescence spectra at room temperature of $SrMoO_4$ powders excited with a 488 nm line of an argon ion laser and deconvolution spectra.

nescence measurements allows to discover the energy levels in the materials and the optical band gap value. UV–vis measurements on the four samples showed a typical value of 3.98 eV. The observed behavior can be associated with the energy difference between the valence band and conduction band for this material.

3.5. Photoluminescence emission at room temperature analysis

Fig. 5 shows the PL spectrum at room temperature of $SrMoO_4$ powders using an exciting wavelength of 488.0 nm. As can be seen in this figure, the general aspect of the PL curve is a broad band covering a large part of the visible spectrum with a maximum situated at 540 nm (green emission). Possibly, the emission profile of this sample can be associated with the contribution of various components. Therefore, to estimate the contribution of each individual component was necessary to deconvolute the PL spectrum.

The deconvolution of the PL spectrum was performed by the PeakFit program (4.05 version) using the Gauss area shape function [34]. The deconvolution results show that the PL profile was better adjusted by adding three peaks. The P_1 peak is situated in the green visible region, the P_2 peak is positioned in the yellow and the P_3 peak is centered in the red wavelength region. Each component represents a different type of electronic transition, which can be linked with the structural arrangement or surface defects. Table 2 shows the obtained parameters in the fit, including position, area and amplitude of each peak individually. The maximum emission of the PL spectra for the sample $SrMoO_4$ occurs in the P_1 peak position (green region). As can be seen, area and amplitude of this component corresponds a 4121.22 (arb. units) and 37.08% of the experimental PL curve, respectively.

Table 2
Results obtained by the deconvolution of the PL curves of $SrMoO_4$ powders obtained by microwave processing at 413 K for 2 h

Sample	$SrMoO_4$
Center of PL maximum emission (nm)	540
Peak-P_1 center (nm)	529
Area of peak-P_1 (%)	37.08
Amplitude of peak-P_1 (arb. units)	4121.42
Peak-P_2 center (nm)	571
Area of peak-P_2 (%)	39.60
Amplitude of peak-P_2 (arb. units)	3255.44
Peak-P_3 center (nm)	627
Area of peak-P_3 (%)	23.32
Amplitude of peak-P_3 (arb. units)	1277.52

Many valid hypotheses are put forward in the literature to explain the possible mechanisms responsible by the emission process of the $SrMoO_4$. Recently, Chen and Gao [35] argued that the green emission is a result of the intrinsic luminescent behavior of the MoO_4^{2-} group. These authors mentioned that the transition of the green luminescence is due $^3T_1, ^3T_2 \rightarrow 1A_1$ transition in the tetrahedral molybdates group. Liu et al. [36] using the microemulsion method showed that PL behavior of $SrMoO_4$ can be modified by the crystallites morphology.

Table 3
Comparative results for $SrMoO_4$ powders obtained by different methods reported in the literature

Method	Form	Temperature (K)	Time (min)	Excitation line (nm)	PL maximum emission (nm)	Reference
Galvanic cell	Film	298	9000	290	485	[16]
Cell electrochemical	Film	286–338	0.13–0.21	230	520	[35]
Microemulsion	Powder	298	60–900	330	390	[36]
Microwave hydrothermal	Powder	413	300	488	540	[This work]

Table 3 presents a comparative of the PL maximum emission of $SrMoO_4$ obtained by different methods reported in the literature.

As can be seen in Table 3, the differences observed in the position of the maximum PL emission in $SrMoO_4$ probably can be associated with the structural organization levels, preparation methods, form and thermal treatment conditions. These factors can be responsible for generating visible color centers in the $SrMoO_4$ lattice and contribute to the PL emission. Moreover, another important factor can be associated with the different excitation wavelengths, which are able to excite different populations of electrons localized in additional energy levels into the band gap.

4. Conclusions

$SrMoO_4$ powders were synthesized by the co-precipitation method and processed in a domestic microwave-hydrothermal. XRD patterns and FT-Raman analyses revealed that obtained powders after MH processing are free of secondary phases and exhibit a single tetragonal structure. Ultraviolet–visible absorption spectroscopy revealed a characteristic optical band gap of 3.98 eV, which is associated with the difference of energy between the valence band and conduction band. Intense PL at room temperature was verified at 540 nm (green emission) under the excitation of 488 nm, which can be associated with the transitions in the tetrahedral $[MoO_4]^{2-}$ group or surface defects.

Acknowledgements

The authors thank the financial support of the Brazilian research financing institutions: CNPq, CAPES, FAPESP and also Prof. Dr. Dawy Keyson-UFPB for adaptation of the hydrothermal reactor in the domestic microwave.

References

[1] Y. Zhang, F. Yang, J. Yang, Y. Tang, P. Yuan, Synthesis of crystalline $SrMoO_4$ nanowires from polyoxometalates, Sol. Stat. Commun. 133 (2005) 759–763.
[2] M. Anicete-Santos, E. Orhan, M.A.M.A. de Maurera, L.G.P. Simões, A.G. Souza, P.S. Pizani, E.R. Leite, J.A. Varela, J. Andrés, A. Beltrán, E. Longo, Contribution of structural order–disorder to the green photoluminescence of $PbWO_4$, Phys. Rev. B 75 (2007) 165105–165115.
[3] J.H. Ryu, J.-W. Yoon, K.B. Shim, Blue luminescence of nanocrystalline $PbWO_4$ phosphor synthesized via a citrate complex route assisted by microwave irradiation, Sol. Stat. Commun. 133 (2005) 657–661.
[4] J.H. Ryu, J.-W. Yoon, C.S. Lim, W.-C. Oh, K.B. Shim, Microwave-assisted synthesis of $CaMoO_4$ nano-powders by a citrate complex method and its photoluminescence property, J. Alloy Compd. 390 (2005) 245–249.
[5] A.P.A. Marques, D.M.A. de Melo, C.A. Paskocimas, P.S. Pizani, M.R. Joya, E.R. Leite, E. Longo, Photoluminescent $BaMoO_4$ nanopowders prepared by complex polymerization method (CPM), J. Sol. Stat. Chem. 179 (2006) 671–678.
[6] H. Fu, J. Lin, L. Zhang, Y. Zhu, Photocatalytic activities of a novel $ZnWO_4$ catalyst prepared by a hydrothermal process, Appl. Catal. A 306 (2006) 58–67.
[7] A.M.E.S. Raj, C. Mallika, O.M. Sreedharan, K.S. Nagaraja, Manganese oxide–manganese tungstate composite humidity sensors, Mater. Lett. 53 (2002) 316–320.
[8] R. Sundaram, K.S. Nagaraja, Electrical and humidity sensing properties of lead(II) tungstates–tungsten(VI) oxide and zinc(II) tungstates–tungsten(VI) oxide composites, Mater. Res. Bull. 39 (2004) 581–590.
[9] R.C. Pullar, S. Farrah, N.M. Alford, $MgWO_4$, $ZnWO_4$, $NiWO_4$ and $CoWO_4$ microwave dielectric ceramics, J. Eur. Ceram. Soc. 27 (2007) 1059–1063.
[10] G. Zhang, R. Jia, Q. Wu, Preparation, structural and optical properties of AWO_4 (A = Ca, Ba, Sr) nanofilms, Mater. Sci. Eng. B 128 (2006) 254–259.
[11] Z. Lou, M. Cocivera, Cathodoluminescence of $CaWO_4$ and $SrWO_4$ thin films prepared by spray pyrolysis, Mater. Res. Bull. 37 (2002) 1573–1582.
[12] I.C. Lekshmi, A. Gayen, M.S. Hegde, The effect of strain on nonlinear temperature dependence of resistivity in $SrMoO_3$ and $SrMoO_{3-x}N_x$ films, Mater. Res. Bull. 40 (2005) 93–104.
[13] A. Kaddouri, E. Tempesti, C. Mazzocchia, Comparative study of β-nickel molybdate phase obtained by conventional precipitation and the sol–gel method, Mater. Res. Bull. 39 (2004) 695–706.
[14] H.H. Wang, D.F. Cui, Y.L. Zhou, Z.H. Chen, F. Chen, T. Zhao, H.B. Lu, G.Z. Yang, M.C. Xu, Y.C. Lan, X.L. Chen, H.J. Qian, F.Q. Liu, Growth and characterization of $SrMoO_3$ thin films, J. Cryst. Growth 226 (2001) 261–266.
[15] J.P. Chu, I.J. Hsieh, J.T. Chen, M.S. Feng, Growth of $MgWO_4$ phosphor by RF magnetron sputtering, Mater. Chem. Phys. 53 (1998) 172–178.
[16] J. Bi, C.-H. Cui, X. Lai, F. Shi, D.-J. Gao, Synthesis of luminescent $SrMoO_4$ thin films by a non-reversible galvanic cell method, Mater. Res. Bull. 43 (2008) 743–747.
[17] J.-H. Lee, C.-K. Kim, S. Katoh, R. Murakami, Microwave-hydrothermal versus conventional hydrothermal preparation of Ni- and Zn-ferrite powders, J. Alloy Compd. 325 (2001) 276–280.
[18] V. Sreeja, P.A. Joy, Microwave-hydrothermal synthesis of α-Fe_2O_3 nanoparticles and their magnetic properties, Mater. Res. Bull. 42 (2007) 1570–1576.
[19] G.J. Wilson, A.S. Matijasevich, D.R.G. Mitchell, J.C. Schulz, G.D. Will, Modification of TiO_2 for enhanced surface properties: finite Ostwald ripening by a microwave hydrothermal process, Langmuir 22 (2006) 2016–2027.
[20] S. Komarneni, M.C. D'Arrigo, C. Leonelli, G.C. Pellacani, H. Katsuki, Microwave-hydrothermal synthesis of nanophase ferrites, J. Am. Ceram. Soc. 81 (1998) 3041–3043.
[21] S. Komarneni, R.K. Rajha, H. Katsuki, Microwave-hydrothermal processing of titanium dioxide, Mat. Chem. Phys. 61 (1999) 50–54.
[22] T. Thongtem, A. Phuruangrat, S. Thongtem, Characterization of $MMoO_4$ (M = Ba, Sr and Ca) with different morphologies prepared using a cyclic microwave radiation, Mater. Lett. 62 (2008) 454–457.
[23] T. Thongtem, A. Phuruangrat, S. Thongtem, Preparation and characterization of nanocrystalline $SrWO_4$ using cyclic microwave radiation, Curr. Appl. Phys. 8 (2008) 189–197.
[24] T.J.B. Holland, S.A.T. Redfern, Unit cell refinement from powder diffraction data: the use of regression diagnostics, Miner. Mag. 61 (1997) 65–77.
[25] http://www.icdd.com/profile/overview.htm.
[26] S.-Y. Wu, H.-N. Dong, W.-H. Wei, Investigations on the local structures and the EPR parameters for Er^{3+} in $PbMoO_4$ and $SrMoO_4$, J. Alloy Compd. 375 (2004) 39–43.
[27] D. Chen, K. Tang, F. Li, H. Zheng, A simple aqueous mineralization process to synthesize tetragonal molybdate microcrystallites, Cryst. Growth Des. 6 (2006) 247–252.
[28] http://www.jcrystal.com/steffenweber/JAVA/JSV/jsv.html.
[29] S. Takai, S. Touda, K. Oikawa, K. Mori, S. Torii, T. Kamiyama, T. Esaka, Powder neutron diffraction study of Ln-substituted $PbWO_4$ oxide ion conductors, Solid State Ionics 148 (2002) 123–133.
[30] E. Grmen, E. Daniels, J.S. King, Crystal structure refinement of $SrMoO_4$, $SrWO_4$, $CaMoO_4$, and $BaWO_4$ by neutron diffraction, J. Chem. Phys. 55 (1971) 1093–1097.

[31] T.T. Basiev, A.A. Sobol, Y.K. Voronko, P.G. Zverev, Spontaneous Raman spectroscopy of tungstate and molybdate crystals for Raman lasers, Opt. Mater. 15 (2000) 205–216.
[32] T.T. Basiev, A.A. Sobol, P.G. Zverev, L.I. Ivleva, V.V. Osiko, R.C. Powell, Raman spectroscopy of crystals for stimulated Raman scattering, Opt. Mater. 11 (1999) 307–314.
[33] D.L. Wood, J. Tauc, Weak absorption tails in amorphous semiconductors, Phys. Rev. B 5 (1972) 3144–3151.
[34] http://www.systat.com/products/PeakFit/.
[35] L. Chen, Y. Gao, Mechanisms and applications of cell electrochemical technique to prepare luminescent $SrMoO_4$ thin films, Chem. Eng. J. 131 (2007) 181–185.
[36] J. Liu, J. Ma, B. Lin, Y. Ren, X. Jiang, J. Tao, X. Zhu, Room temperature synthesis and optical properties of $SrMoO_4$ crystallites by w/o microemulsion, Ceram. Int. (2007) in press.